BIOCHEMISTRY
including biophysical chemistry & molecular biology

Article

pubs.acs.org/biochemistry

The Human ZIP4 Transporter Has Two Distinct Binding Affinities and Mediates Transport of Multiple Transition Metals

Sagar Antala and Robert E. Dempski*

Department of Chemistry and Biochemistry, Worcester Polytechnic Institute, 100 Institute Road, Worcester, Massachusetts 01605, United States

ABSTRACT: Zinc is the second most abundant transition metal in the body. Despite the fact that hundreds of biomolecules require zinc for proper function and/or structure, the mechanism of zinc transport into cells is not well-understood. The ZIP (Zrt- and Irt-like proteins; SLC39A) family of proteins acts to increase cytosolic concentrations of zinc. Mutations in one member of the ZIP family of proteins, the human ZIP4 (hZIP4; SLC39A4) protein, can result in the disease *acrodermatitis enteropathica* (AE). AE is characterized by growth retardation and diarrhea, as well as behavioral and neurological disturbances. While the cellular distribution of hZIP4 protein expression has been elucidated, the cation specificity, kinetic parameters of zinc transport, and residues involved in cation translocation are unresolved questions. Therefore, we have established a high signal-to-noise zinc uptake assay following heterologous expression of hZIP4 in *Xenopus laevis* oocytes. The results from our experiments have demonstrated that zinc, copper(II), and nickel can be transported by hZIP4 when the cation concentration is in the micromolar range. We have also identified a nanomolar binding affinity where copper(II) and zinc can be transported. In contrast, under these conditions, nickel can bind but is not transported by hZIP4. Finally, labeling of hZIP4 with maleimide or diethylpyrocarbonate indicates that extracellularly accessible histidine, but not cysteine, residues are required, either directly or indirectly, for cation uptake. The results of our experiments identify at least two coordination sites for divalent cations and provide a new framework for investigating the ZIP family of proteins.

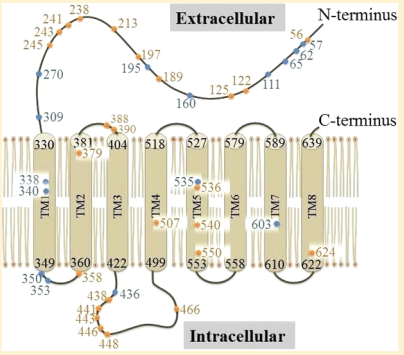

Zinc is the second most abundant transition metal found in eukaryotic organisms and is an essential trace element for maintaining cell homeostasis.[1−3] While there is approximately 2 g of zinc in an adult human, only 10% is metabolically active.[2] Zinc is important for enzyme catalysis (alcohol dehydrogenase) and the structural integrity of proteins (zinc fingers); it also plays a role in cell regulation (transcription factors and cell signaling).[3] It is the only metal ion that can interact with all six classes of enzymes (oxidoreductases, transferases, hydrolases, lyases, isomerases, and ligases), defining its importance in various cellular events.[1] Part of the wide versatility of zinc is due to the fact that zinc can have a wide range of coordination geometries, is a fast ligand exchanger, and does not have redox properties under physiological conditions.[4,5] The lack of redox properties separates zinc from other transition metals such as iron and copper, as zinc is less likely to cause oxidative damage in vivo.[5]

The mechanism of zinc uptake, intracellular transport, and export is a complex field that is largely unexplored.[6] Zinc transport was initially hypothesized to be mediated by cotransport with either cysteine or histidine, as zinc binds these amino acid residues with high affinity.[7] However, this possibility was discredited in 1995, when the first mammalian zinc transporter gene was identified.[2,4] Subsequent studies have identified two classes of zinc transporters: those that mediate a net increase (ZIP; Zrt- and Irt-like proteins; SLC39A) and those that mediate a net decrease (Znt; solute-linked carrier 30; SLC30A) in cytosolic zinc levels.[6,8] The mammalian ZnT family is comprised of 10 member proteins, whereas the mammalian ZIP family has 14 member proteins.[9] Elucidation of the crystal structure of the bacterial efflux zinc transporter YiiP, with a sequence 25−30% homologous with that of mammalian ZnT zinc transporters, has provided important insight into this class of protein.[10] An analysis of the YiiP crystal structure demonstrated that Zn^{2+} was coordinated by histidine residues within the transmembrane domains.[10]

While the tissue distribution of these proteins has been investigated, the mechanism of many of these proteins is not well-understood.[6] The best characterized human ZIP proteins are hZIP8, hZIP13, and hZIP14.[11,12] hZIP8 has been shown to be a divalent cation/HCO_3^- transporter that can transport Zn^{2+} and Cd^{2+}, while hZIP13 has been shown to transport Zn^{2+} into the Golgi.[12,13] In contrast, hZIP14 has been shown to transport Mn^{2+} in addition to Zn^{2+} and Cd^{2+}.[11] Finally, the protein ZIPB from *Bordetella bronchiseptica* is the first ZIP homologue to be purified and functionally reconstituted.[14] An analysis of the results from these experiments has demonstrated that this protein can transport Zn^{2+} and Cd^{2+}, but not other divalent transition metals. Combined, these data suggest that each member of the hZIP family of proteins could have transport capabilities beyond zinc that may vary for each member of the hZIP family of proteins.

To date, the most studied ZIP4 protein was derived from mouse (mZIP4). The sequence of hZIP4 is ∼70% homologous with that of mZIP4. The transmembrane domains of hZIP4 and

Received: October 7, 2011
Revised: January 11, 2012
Published: January 11, 2012

ACS Publications © 2012 American Chemical Society

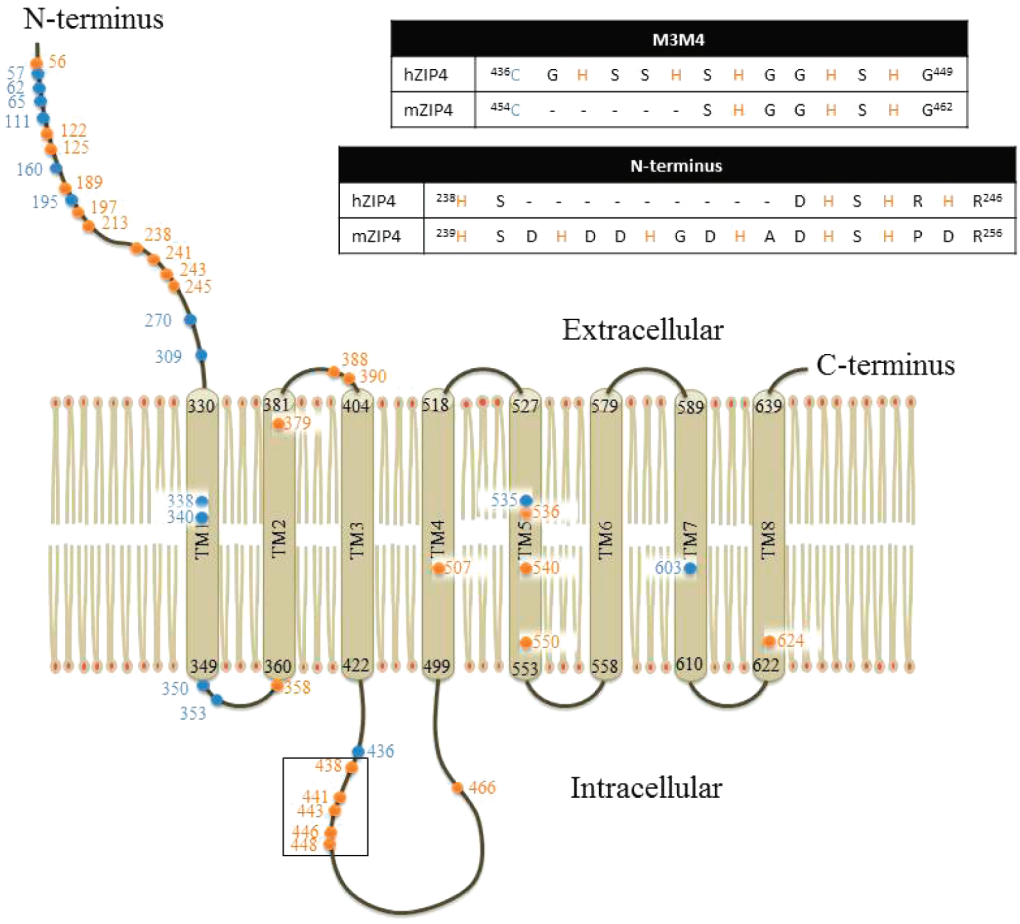

Figure 1. Predicted schematic diagram of the human ZIP4 protein. The full-length protein is displayed where histidine residues are shown as orange circles and cysteine residues as blue circles. The first and last residues of the transmembrane domains, as predicted by hydropathy analysis, are shown. A comparison of the histidine-rich regions between the mouse and human ZIP4 in the N-terminal domain as well in the loop between transmembranes 3 and 4 (M3M4) are listed in the table.

mZIP4 are highly conserved.[15] However, there are some key differences between these two proteins. First, the N-terminal domains of mZIP4 and hZIP4 are only 68% identical, and the histidine-rich, putative extracellular zinc binding domain is not conserved (Figure 1). Second, the histidine-rich, putative intracellular zinc binding domain is not conserved between mZIP4 and hZIP4. From a functional standpoint, it has been suggested that mZIP4 is a zinc-selective transporter, because zinc transport is not substantially inhibited by the addition of a 50-fold excess of other transition metals.[15]

The hZIP4 protein has two major isoforms. The most abundant isoform is 647 amino acids long. The second major isoform is 622 amino acids long. In mouse, the predominant species is the longer isoform.[15] hZIP4 has eight transmembrane domains with both N- and C-termini facing the extracellular side (Figure 1).[16,17] The N-terminus of hZIP4 is comprised of 327 amino acids. This domain is rich in histidine and cysteine, suggesting possible residues for zinc coordination. Furthermore, it has been observed that when the cellular concentration of zinc is high, hZIP4 undergoes protein ubiquitination and subsequent degradation.[18] It has been shown that mutagenesis of all the histidine residues (except His^{466}) within the loop between transmembranes 3 and 4 eliminates hZIP4 ubiquitination.[18] This suggests a direct role between coordination of zinc to this domain and the cell surface regulation of hZIP4.

hZIP4 is expressed in the small intestine, stomach, colon, cecum, and kidney.[16] Several mutations within this protein have been correlated to the lethal autosomal recessive pediatric disorder *acrodermatitis enteropathica* (AE).[19] AE is a zinc transport disease.[19] Symptoms of AE include growth retardation, diarrhea, and behavioral and neurological disturbances, which can be reversed with a diet rich in zinc.[20] More recently, it has been demonstrated that hZIP4 is overexpressed in pancreatic cancer, and the amount of hZIP4 on the cell surface is directly proportional to the metastatic stage of this disease.[21] Pancreatic cancer is the fourth leading cause of cancer-related deaths in the United States, with an overall survival rate of less than one year.[22] While the increase in the level of surface expression of hZIP4 in pancreatic cancer cells could be a result of carcinogenesis, artificially increasing the level of surface expression of hZIP4 using a retrovirus increases the level of expression of a series of proteins that are known to contribute to the onset and progression of pancreatic cancer.[23−26] Therefore, it appears that the surface expression of hZIP4 directly regulates the expression of proteins known to be involved in the initiation and progression of pancreatic cancer.

Considering the key role of hZIP4 in human zinc homeostasis as well as in the initiation and progression of pancreatic cancer combined with earlier results that have demonstrated differing cation selectivity for the ZIP family of proteins, our objective has

dx.doi.org/10.1021/bi201553p | *Biochemistry* 2012, 51, 963−973

been to elucidate the cation specificity of hZIP4. Therefore, we have developed a radioisotope uptake assay following expression of hZIP4 in *Xenopus laevis* oocytes. We have also investigated which extracellular accessible residues are important for zinc uptake. The results from these experiments provide novel insight into the function of hZIP4 while introducing a series of unresolved questions with regard to the mechanism of cation transport.

EXPERIMENTAL PROCEDURES

Reagents. The SLC39A4 (hZIP4) gene and the mMessage mMachine SP6 kit were purchased from Invitrogen (Carlsbad, CA). Restriction enzymes were purchased from New England Biolabs, Inc. (Ipswich, MA). The radioisotopes $^{65}ZnCl_2$, $^{63}NiCl_2$, and $^{64}CuCl_2$ were obtained from Perkin-Elmer (Waltham, MA), Oak Ridge National Laboratories (Oak Ridge, TN), and Washington University of St. Louis (St. Louis, MO), respectively. Maleimide was purchased from Alfa Aesar, Inc. (Ward Hill, MA). All other chemicals were obtained from Sigma-Aldrich Corp. (St. Louis, MO) unless otherwise indicated.

Plasmid Construct. The hZIP4 gene, containing 647 residues, was subcloned, with a Strep tag (WSHPQPEK) at the C-terminus, into the *X. laevis* oocyte pTLN vector.[27] The two unique restriction sites, *Nco*I at the N-terminus and *Bgl*II at the C-terminus, were used for unidirectional insert incorporation. The entire hZIP4-Strep tag sequence was verified by DNA sequencing.

Preparation of *X. laevis* Oocytes for in Vitro Expression of hZIP4. Oocytes were surgically removed and isolated from *X. laevis* following a protocol approved by the Worcester Polytechnic Institute Animal Care and Use Committee. In brief, female *X. laevis* frogs were anesthetized with tricaine (1.5 g/L for 1 h). Oocytes were extracted by partial ovariectomy and were digested with 2 mg/mL collagenase in ORI buffer [90 mM NaCl, 2 mM KCl, 2 mM $CaCl_2$, and 5 mM MOPS (pH 7.4)] for 4−5 h at 18 °C on an orbital shaker.[28] After digestion, oocytes were incubated with Ca^{2+}-free ORI buffer [90 mM NaCl, 2 mM KCl, and 5 mM MOPS (pH 7.4)] for 10 min. Following this step, the oocytes were washed exhaustively, first, with Ca^{2+}-free ORI buffer and, second, with ORI buffer. Oocytes were stored at 18 °C in ORI buffer with 20 μg/mL gentamycin until they were needed.

In Vitro Expression of hZIP4. The pTLN plasmid containing the full-length hZIP4 gene with a Strep tag was linearized with *Mlu*I and purified using the High Pure PCR Product Purification Kit (Roche Applied Science, Indianapolis, IN). mRNA was prepared and purified using the SP6 mMessage mMachine kit according to the manufacturer's instructions. Purified mRNA was quantified on a NanoDrop ND-2000c spectrophotometer (Thermo Scientific, Rochester, NY). A 25 ng aliquot of mRNA in 50 nL of DEPC-treated H_2O was injected into each oocyte and incubated at 18 °C in ORI buffer with 20 μg/mL gentamycin for 3 days prior to measurements. For negative controls, 50 nL of DEPC H_2O was injected into oocytes.

Uptake Assay. Uptake experiments were loosely based on established protocols.[29] Oocytes, injected with either hZIP4 mRNA or DEPC H_2O, were washed and preincubated in 750 μL of uptake buffer [90 mM NaCl, 10 mM HEPES, and 1 mM ascorbic acid (pH 7.4)] for 30 min. The uptake assay was initiated upon addition of a radioisotope ($^{63}NiCl_2$, $^{64}CuCl_2$, or $^{65}ZnCl_2$) and was quenched by removal of five to eight oocytes into cold uptake buffer followed by extensive washes. All $^{64}CuCl_2$ uptake assays were performed in the absence of ascorbic acid. Under these experimental conditions, copper is predominantly in the +2 oxidation state as determined using the copper-bathocuproinedisulfonic acid standard absorbance assay. Each oocyte was solubilized by being vigorously vortexed in 1% (w/v) sodium dodecyl sulfate (SDS). Total radioactivity was measured using a Beckman LS6500 Multi-Purpose Scintillation Counter with Scintisafe-30% liquid scintillation cocktail (Fisher Scientific, Pittsburgh, PA). Counts from DEPC H_2O-injected oocytes were subtracted from hZIP4 mRNA-injected oocytes unless otherwise indicated. Counts per minute (cpm) were converted to picograms (pg) or femtograms (fg) using the following equation:

$$\text{amount (pg or fg)} = \frac{\text{cpm} \times \text{dilution factor} \times \text{half-life correction factor}}{\text{specific activity(dpm/pg or fg)} \times \text{efficiency}}$$

where cpm values were the raw data obtained from each oocyte, dilution factor is the total concentration of radioactive and nonradioactive metal ion divided by the concentration of radioactive cation, half-life correction factor is the half-life of the radioisotope divided by the half-life of the radioisotope minus time elapsed, and the specific activity [in disintegrations per minute (dpm)/pg or fg] is provided by the manufacturer. The half-lives for $^{63}Ni^{2+}$, $^{64}Cu^{2+}$, and $^{65}Zn^{2+}$ are 100 years, 12.7 h, and 244 days, respectively. For a more accurate conversion of cpm to dpm, it was experimentally determined that the efficiency of our scintillation fluid/counter for $^{63}Ni^{2+}$ was 74.3% while the efficiency for $^{64}Cu^{2+}$ and $^{65}Zn^{2+}$ was 68.4%.

Data were fit to the equation

$$y = \frac{V_{max}[X^{2+}]^n}{K_m{}^n + [X^{2+}]^n}$$

where V_{max} is the maximal velocity, $[X^{2+}]$ is the concentration of a divalent metal ion, K_m is the concentration of divalent metal at one-half V_{max}, and n is the Hill coefficient.

Immunofluorescence Microscopy. Oocytes, 3 days postinjection with hZIP4 mRNA (preincubated with 0 or 10 μM $ZnCl_2$ for 1 h in uptake assay buffer) or DEPC H_2O, were washed and fixed in a 4% (w/v) paraformaldehyde solution for 20 min at room temperature. Oocytes were washed with phosphate-buffered saline (PBS) two times and cryoprotected in 30% (w/v) sucrose in PBS overnight at 4 °C. The oocytes were frozen in OCT medium (Tissue-Tek) and cut into 25 μm sections. The sections were mounted on positively charged slides (VWR Micro Slides) and blocked in a 5% BSA solution in PBS for 1 h at room temperature. The oocyte sections were washed with PBS two times and incubated with Strep-tectin antibody (IBA Biotagnology) conjugated with Chromeo488 dye for 1 h at 37 °C. The sections were washed with PBS two times and then mounted in fluorescence protective mounting medium (KPL Mounting Medium). Fluorescence images were taken using a Leica DM LB-2 microscope with a 20× objective.

Maleimide and DEPC Labeling of hZIP4. Oocytes were preincubated for 30 min in varying concentrations of either DEPC or maleimide. Prior to initiation of the uptake assay with $^{65}ZnCl_2$, half of the oocytes were washed with cold uptake buffer. Initiation of the reaction, quenching, and radioisotope quantification were performed as described above. To determine whether exposure to DEPC is toxic to the oocytes, the resting membrane protential was determined using a TEC 03X Standard System two-electrode voltage clamp setup (NPI Electronics, Tamm, Germany).

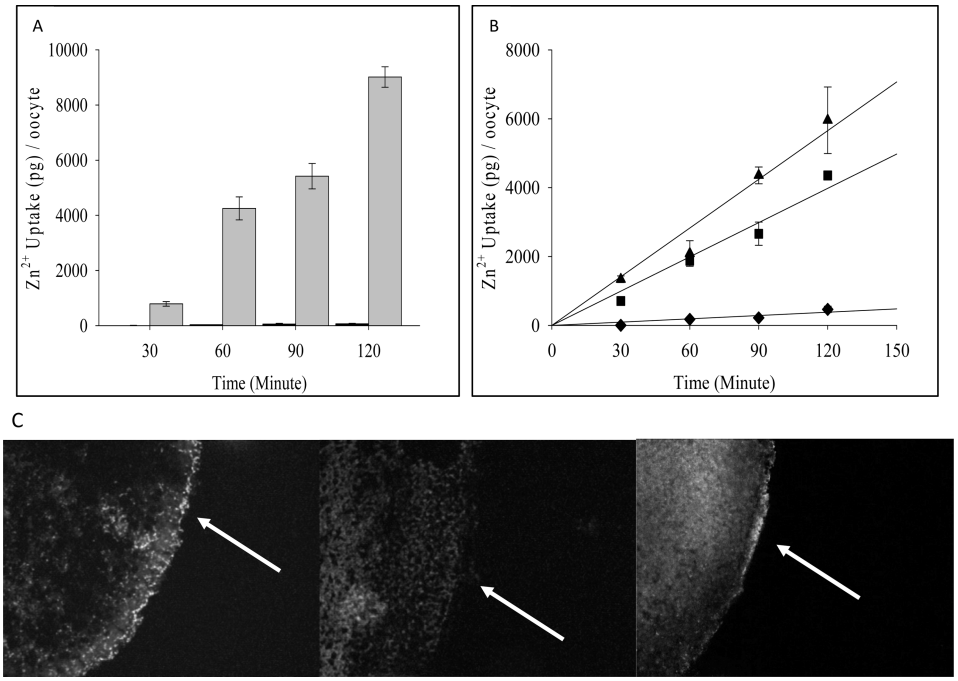

Figure 2. $^{65}Zn^{2+}$ radioisotope uptake. (A) Oocytes were injected with either 50 ng of mRNA of hZIP4-Strep in 50 nL of DEPC H_2O or 50 nL of DEPC H_2O. Three days postinjection, $^{65}Zn^{2+}$ uptake was measured as described in Experimental Procedures over the course of 2 h. Oocytes were removed every 30 min for a total of four time points. A final $^{65}Zn^{2+}$ concentration of 21.75 μM was used for this experiment. Radioisotope uptake is shown for DEPC H_2O-injected (black) and hZIP4-Strep mRNA-injected (gray) oocytes. Counts per minute were converted to picograms of $^{65}Zn^{2+}$. Data originated from five to eight oocytes; values are means ± SEM. (B) Oocytes, injected with 25 ng of hZIP4-Strep mRNA, were incubated with varying amounts of $ZnCl_2$ [(◆) 0.49 μM Zn^{2+}, (■) 44.7 μM Zn^{2+}, and (▲) 105.1 μM Zn^{2+}]. The assay was quenched every 30 min up to 120 min, and data originated from five to eight oocytes; values are means ± SEM. In this and all other figures, the error bars were omitted when they were smaller than the symbols. (C) Representative images of three oocytes injected with hZIP4 mRNA tagged with a Strep tag on the C-terminus and probed with Chromeo488-conjugated anti-Strep antibody. Anti-Strep specific staining is present in oocytes injected with hZIP4 mRNA before (left) and after (right) exposure to 10 μM $ZnCl_2$. No staining is observed in DEPC H_2O-injected oocytes (center). The arrow indicates the surface of the oocyte.

RESULTS

hZIP4-Mediated Zinc Uptake. Following insertion of the full-length hZIP4 gene with the Strep tag added onto the C-terminus into the pTLN vector and mRNA synthesis, our initial objective was to generate a zinc uptake assay with a high specificity and a robust signal-to-noise ratio. The longer, 647-amino acid protein was investigated throughout the course of these experiments as it has been shown that the homologous longer protein is the predominant species in mice.[15] *Xenopus* oocytes were injected with varying amounts of hZIP4-Strep mRNA, and radioactive $^{65}Zn^{2+}$ uptake was measured 3−6 days postinjection. During the course of all assays, DEPC H_2O was injected for negative controls. Optimal radioisotope uptake was observed following injection of 50 ng of mRNA of hZIP4 where the assay was initiated 3 days post-mRNA injection (Figure 2A). It was observed during the course of these experiments that injection of a larger amount of hZIP4 mRNA resulted in a decreased viability of oocytes after an incubation period of 3 days.

Following optimization of the amount of hZIP4-Strep mRNA to inject into oocytes and identification of the best time following injection to measure radioisotope uptake, we were interested in determining the range of zinc concentrations that would result in a linear amount of radioisotope uptake over time. Therefore, we initiated the uptake assay using a final $ZnCl_2$ concentration from 0.49 to 105.1 μM (Figure 2B). The results from these experiments demonstrated that zinc uptake is roughly linear over 2 h over this range of zinc concentrations and that zinc uptake is proportional to the amount of Zn^{2+} in the uptake assay. To establish the localization of the heterologously expressed hZIP4 in *X. laevis* oocytes, we detected expression of hZIP4 in sections of paraformaldehyde-fixed oocytes using a Chromeo488-labeled anti-Strep antibody. Immunofluorescence was observed in mRNA-injected oocytes before and after exposure to 10 μM $ZnCl_2$, but not visible in DEPC H_2O-injected controls, demonstrating localization of hZIP4 protein at the plasma membrane (Figure 2C).

Determination of K_m and V_{max} for hZIP4-Mediated Zinc Uptake. Our next objective was to determine the K_m for the transport of zinc by hZIP4. Therefore, we measured Zn^{2+} uptake with varying concentrations of the radioisotope in the uptake assay buffer for 60 min. Under our experimental conditions, two distinct K_m values for zinc could be elucidated. In both cases, zinc uptake was plotted as a function of the concentration of zinc in the assay buffer (Figure 3A,B).

An analysis of the results of our experiments demonstrated that at low zinc concentrations, the K_m was 76 ± 5 nM, where n = 3.6 ± 0.6 and V_{max} = 94 ± 6 pg oocyte^{-1} h^{-1}. A second K_m for zinc was calculated in the micromolar range at 1.4 ± 0.3 μM, where n = 1.2 ± 0.3 and V_{max} = 850 ± 60 pg oocyte^{-1} h^{-1} (Figure 3B). Our results demonstrated that V_{max} varied for each experiment. This is directly attributable to changes in surface expression of hZIP4 in oocytes. However, the values for K_m and n were consistent over a series of repeated experiments at both micromolar and nanomolar zinc concentrations.

dx.doi.org/10.1021/bi201553p | *Biochemistry* 2012, 51, 963−973

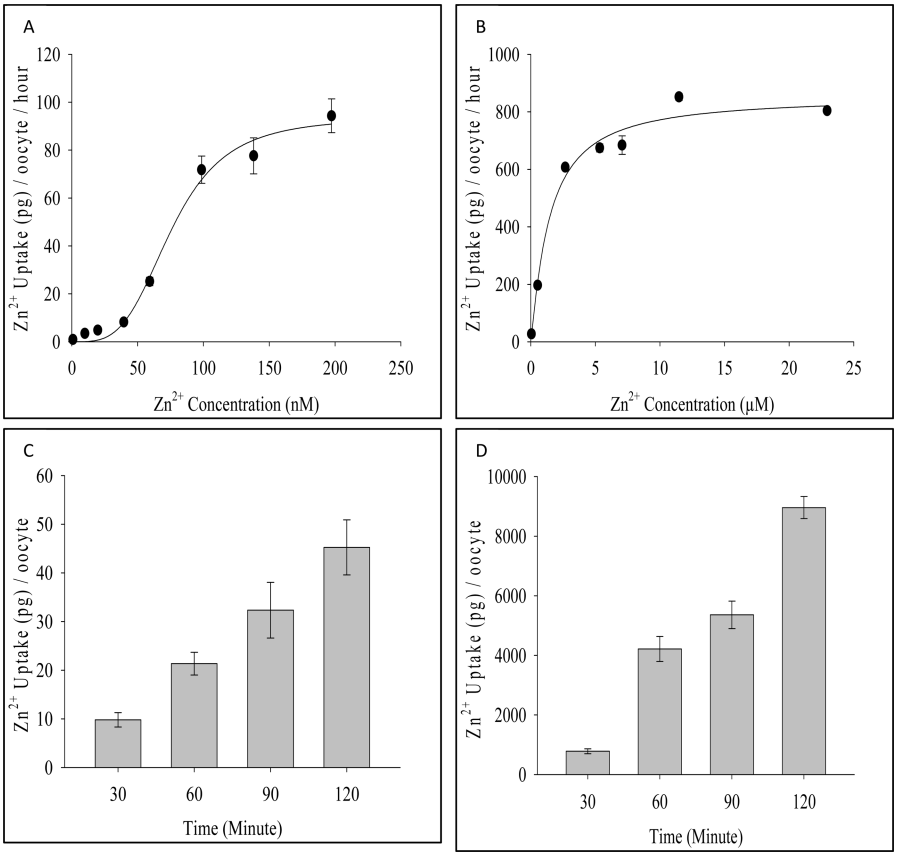

Figure 3. Transport parameters, K_m and V_{max}, for hZIP4 were elucidated at low (A) and high (B) concentrations of zinc by measuring the amount of Zn^{2+} taken up by oocytes injected with hZIP4-Strep mRNA over 1 h in assay buffer that contained varying amounts of $ZnCl_2$. The data were fit to the Michaelis–Menten equation described in the text, and data originated from five to eight oocytes; values are means ± SEM. At low concentrations, K_m and n were calculated to be 76 ± 5 nM and 3.6 ± 0.6, respectively, whereas at high concentrations, K_m was found to be 1.4 ± 0.3 μM and n to be 1.2 ± 0.3. The rate of uptake of Zn^{2+} into oocytes was measured as a function of time at 82 nM (C) and 21.75 μM (D) over the course of 2 h. The assay was quenched every 30 min up to 120 min, and data originated from five to eight oocytes; values are means ± SEM.

To elucidate the rate of hZIP4-mediated zinc uptake in the range of both K_m values, zinc uptake was measured as a function of time in the nanomolar and micromolar range (82 nM and 21.75 μM Zn^{2+} in panels C and D of Figure 3, respectively). Under both of these conditions, we observed an approximately linear increase in the level of zinc uptake over the course of the 2 h experiment. In addition, the difference in radioactivity when zinc uptake was measured in the nanomolar concentration was at least 4 times higher in the mRNA-injected oocytes than in the DEPC H_2O-injected oocytes.

Competition of Zinc Uptake with Additional Transition Metals. To date, the cation specificity of 3 of the 14 human ZIP proteins has been examined.[30−32] These proteins have unique transport properties despite the fact that the primary sequences of these proteins are highly homologous. Therefore, we hypothesized that hZIP4 might transport cations other than zinc. To test this hypothesis, our first objective was to determine whether any divalent cations would inhibit hZIP4-mediated $^{65}Zn^{2+}$ uptake. While this is not a direct measurement of cation transport, this experiment would provide insight into which cations should be tested for hZIP4-mediated cation uptake. For this experiment, 600 μM of various transition metals were preincubated with oocytes expressing hZIP4. As a positive inhibition control, 600 μM cold Zn^{2+} was preincubated with oocytes expressing hZIP4. The zinc uptake assay was initiated upon addition of 3 μM $^{65}Zn^{2+}$, and the length of time for the uptake assay was 1 h. Uptake of $^{65}Zn^{2+}$ was measured. All of the data were normalized to $^{65}Zn^{2+}$ uptake in the absence of any competing metal. It was expected that cation(s) that inhibited or competed with zinc uptake would decrease the rate of $^{65}Zn^{2+}$ uptake. In contrast, cations that did not inhibit or compete with hZIP4-mediated $^{65}Zn^{2+}$ uptake would demonstrate no change in $^{65}Zn^{2+}$ uptake.

The results from our experiments demonstrated that addition of 600 μM cold Zn^{2+} inhibited 96 ± 1% of $^{65}Zn^{2+}$ uptake (Figure 4). Addition of 600 μM divalent cations Ba^{2+}, Cd^{2+}, Co^{2+}, Fe^{2+}, Mg^{2+}, and Mn^{2+} had no significant effect on $^{65}Zn^{2+}$ uptake. In contrast, addition of 600 μM Cu^{2+} or Ni^{2+} decreased the rate of hZIP4-mediated $^{65}Zn^{2+}$ uptake. The addition of 600 μM Ni^{2+} inhibited 35 ± 8% of $^{65}Zn^{2+}$ uptake, while the addition of 600 μM Cu^{2+} inhibited 96 ± 1% of $^{65}Zn^{2+}$ uptake.

Affinity of Nickel for hZIP4. Considering that our competition experiment does not directly test for cation uptake other than zinc, our next objective was to directly measure whether Cu^{2+} or Ni^{2+} could be transported by hZIP4. Therefore, $^{63}Ni^{2+}$ uptake was measured using our established uptake assay except that $^{65}Zn^{2+}$ was replaced with $^{63}Ni^{2+}$. As a first step, we examined whether nickel uptake was linear over time. At low concentrations (4.76 nM $^{63}Ni^{2+}$), there is a measurable amount of nickel that accumulates with the hZIP4-injected oocytes that does not increase over the 2 h uptake assay (Figure 5A). In contrast, when the concentration of Ni^{2+} is increased in the

dx.doi.org/10.1021/bi201553p | *Biochemistry* 2012, 51, 963−973

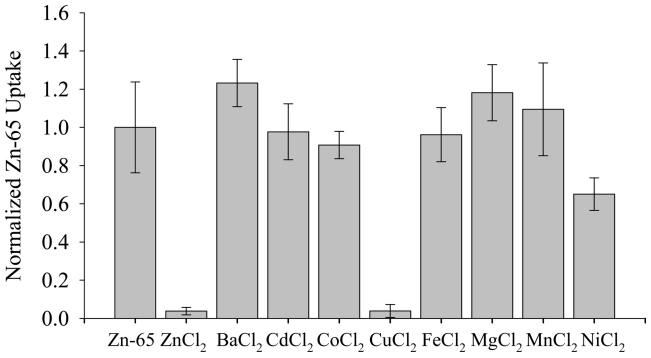

Figure 4. Competition of $^{65}Zn^{2+}$ uptake with a series of divalent cations. To determine which divalent cations inhibited hZIP4-mediated $^{65}Zn^{2+}$ uptake, oocytes expressing hZIP4 were preincubated in 600 μM cold $ZnCl_2$, $BaCl_2$, $CdCl_2$, $CoCl_2$, $CuCl_2$, $FeCl_2$, $MgCl_2$, $MnCl_2$, or $NiCl_2$ in uptake assay buffer. The uptake assay was initiated by adding 3.0 μM $^{65}ZnCl_2$. The assay was quenched after 1 h as described in Experimental Procedures. Data were normalized to the amount of $^{65}Zn^{2+}$ uptake in the absence of a competing cation, and data originated from five to eight oocytes; values are means ± SEM.

uptake assay (5.25 μM), nickel uptake is approximately linear over 2 h (Figure 5B).

After obtaining these results, we next performed experiments with a goal of determining the K_m of Ni^{2+} at both nanomolar and micromolar concentrations. When our uptake assay contained nanomolar concentration of $^{63}Ni^{2+}$, an analysis of our experiments determined that nickel uptake follows Michaelis–Menten kinetics, where K_m = 1.1 ± 0.1 nM, n = 1.3 ± 0.1, and V_{max} = 102 ± 4 fg oocyte^{-1} h^{-1} (Figure 5C). In the micromolar Ni^{2+} range, an analysis of our experiments revealed that K_m = 2.9 ± 0.3 μM, n = 1.5 ± 0.2, and V_{max} = 95 ± 5 pg oocyte^{-1} h^{-1} (Figure 5D). In addition, the difference in radioactivity when nickel uptake was measured at the nanomolar concentration was at least 4 times higher in the mRNA-injected oocytes than in the DEPC H_2O-injected oocytes.

Parameters of Copper(II) Transport. Considering our experimental result that a 200-fold excess of Cu^{2+} inhibits more than 95% of $^{65}Zn^{2+}$ uptake, our goal was to directly examine Cu^{2+} uptake. In a manner similar to that used in the previous experiments, the first step for these experiments was to measure the rate of Cu^{2+} uptake at low (6.6 nM) and high (10 μM) concentrations (Figure 6A,B). Under each of these conditions, the amount of Cu^{2+} uptake increased at an approximately linear rate during the 2 h experiment. Therefore, our next experiment was to calculate the K_m for Cu^{2+} uptake. Similar to the case for both zinc and nickel, we could elucidate two distinct K_m values

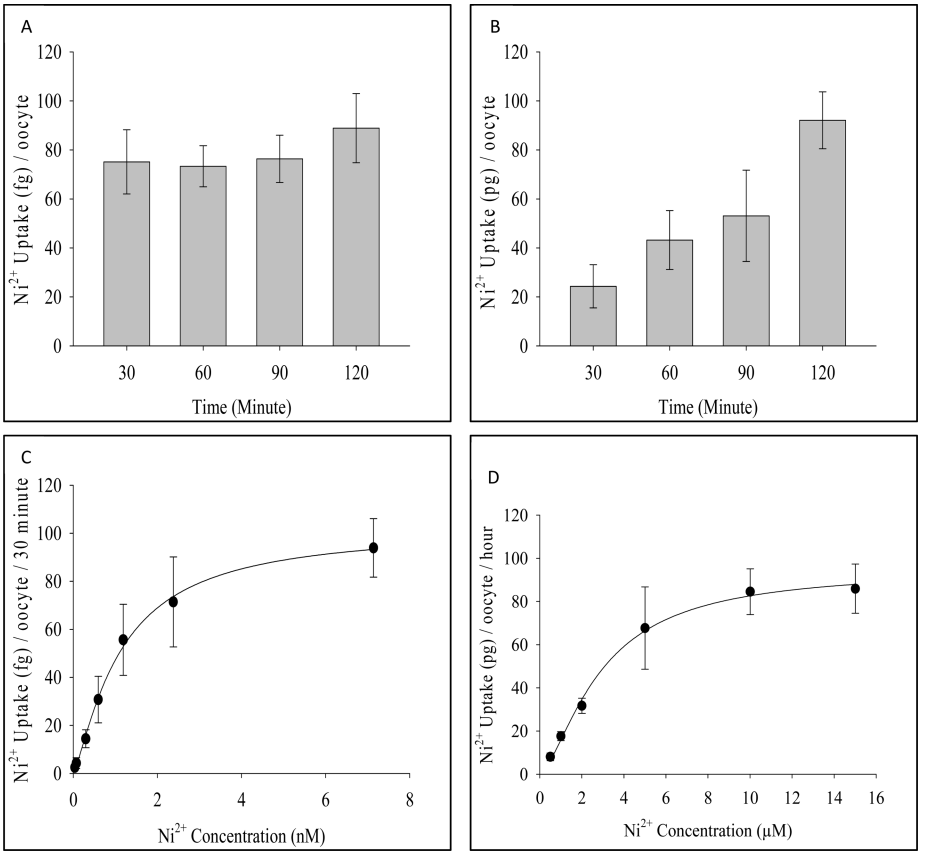

Figure 5. Nickel affinity and transport by hZIP4. (A) Oocytes were injected with either 25 ng of mRNA of hZIP4-Strep in 50 nL of DEPC H_2O or 50 nL of DEPC H_2O. Three days postinjection, $^{63}Ni^{2+}$ uptake was measured as described in Experimental Procedures over the course of 2 h using a final $^{63}NiCl_2$ concentration of 4.76 nM. Oocytes were removed every 30 min for a total of four time points. Radioisotope uptake is shown for hZIP4-Strep mRNA-injected oocytes. Data originated from five to eight oocytes; values are means ± SEM. (B) In a similar manner, Ni^{2+} uptake was measured using a final $NiCl_2$ concentration of 5.25 μM. (C) The K_m and V_{max} of $^{63}Ni^{2+}$ were elucidated at nanomolar $^{63}Ni^{2+}$ concentrations. The data were fit to the Michaelis–Menten equation, where K_m = 1.1 ± 0.1 nM and n = 1.3 ± 0.1. Counts per minute were converted to femtograms of $^{63}Ni^{2+}$. (D) The K_m and V_{max} of Ni^{2+} were elucidated at micromolar Ni^{2+} concentrations. The data were fit to the Michaelis–Menten equation, where K_m = 2.9 ± 0.3 μM and n = 1.5 ± 0.2. Counts per minute were converted to picograms of Ni^{2+}.

dx.doi.org/10.1021/bi201553p | *Biochemistry* 2012, 51, 963–973

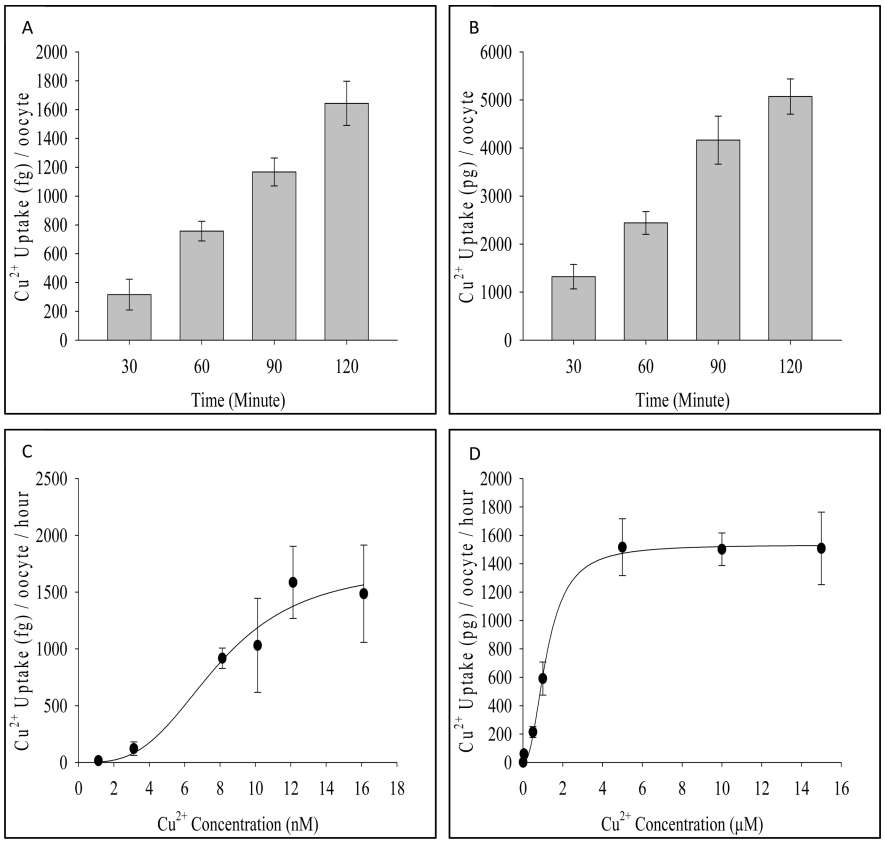

Figure 6. Time course and kinetics of hZIP4-mediated Cu^{2+} uptake. (A) Cu^{2+} uptake was measured over 2 h at a final concentration of 6.6 nM. Data originated from five to eight oocytes; values are means ± SEM. Counts per minute were converted to femtograms of Cu^{2+}. (B) Cu^{2+} uptake was measured at a final concentration of 10 μM over 2 h. Data originated from five to eight oocytes; values are means ± SEM. Counts per minute were converted to picograms of Cu^{2+}. (C) Cu^{2+} uptake was measured after 1 h at varying concentrations of Cu^{2+} to quantify the transport properties of this cation. The data were fit to the Michaelis–Menten equation, where K_m = 8 ± 1 nM and n = 3 ± 2. Counts per minute were converted to femtograms of Cu^{2+}. (D) $^{64}Cu^{2+}$ uptake was measured after 1 h at micromolar concentrations of $^{64}Cu^{2+}$ to quantify the transport properties. At these concentrations, the data were fit to the Michaelis–Menten equation, where K_m = 1.2 ± 0.1 μM and n = 2.2 ± 0.3. Counts per minute were converted to picograms of Cu^{2+}.

for copper uptake when the uptake was plotted as a function of Cu^{2+} concentration. Furthermore, the difference in radioactivity when copper(II) uptake was measured at the nanomolar concentration was at least 4 times higher in the mRNA-injected oocytes than in the DEPC H_2O-injected oocytes. We were able to calculate a K_m of 8 ± 1 nM, where n = 3 ± 2 and V_{max} = 1700 ± 400 fg oocyte^{-1} h^{-1} when Cu^{2+} was added to the uptake assay in nanomolar amounts (Figure 6C). Using a higher concentration of Cu^{2+}, the K_m was calculated to be 1.20 ± 0.09 μM, where n = 2.2 ± 0.3 and V_{max} = 1530 ± 30 pg oocyte^{-1} h^{-1} (Figure 6D).

Extracellular Residues That Mediate $^{65}Zn^{2+}$ Transport. It was initially hypothesized that transport of zinc into cells was mediated by cotransport with either histidine or cysteine residues as zinc binds with high affinity to these residues. This theory was disproved when the first mammalian zinc transporter gene was identified in 1995.[33] On the basis of this initial hypothesis and the fact that zinc coordinates tightly to both cysteine and histidine, we hypothesized that covalent labeling of extracellular accessible cysteine and/or histidine residues would disrupt $^{65}Zn^{2+}$ uptake.

Maleimide and DEPC have been used previously to examine the role of extracellular accessible cysteine and histidine residues, respectively, following heterologous expression in *X. laevis* oocytes.[34,35] Oocytes, injected with either hZIP4 mRNA or DEPC H_2O, were preincubated with maleimide and DEPC H_2O for 30 min. The oocytes were then washed exhaustively with uptake assay buffer, and the uptake assay was initiated upon addition of $^{65}Zn^{2+}$. Under these experimental conditions, no free maleimide or DEPC was present in the uptake assay. No change in zinc uptake was observed following labeling with 1 or 10 mM maleimide (Figure 7). In contrast, while no change was observed in $^{65}Zn^{2+}$ uptake with 1 mM DEPC, a significant decrease in the rate of zinc uptake was observed following labeling of oocytes expressing hZIP4 with 10 mM DEPC.

To further explore the relationship between zinc uptake and labeling of free cysteine and histidine residues, we did not wash out maleimide and DEPC prior to the uptake assay. Therefore, free maleimide or DEPC is available to react with residues in hZIP4 that may move from an inaccessible to an accessible state during the conformational change of hZIP4 that is correlated with zinc transport. Under these conditions, there was an increase in the rate of zinc uptake when 1 mM maleimide was present in the uptake assay during zinc transport. This increase in the rate of zinc uptake in the presence of malemide was abolished when the concentration of maleimide was increased to 10 mM. No significant change in zinc uptake was observed when 1 mM DEPC was present in the uptake assay. In contrast, there was a significant decrease in the rate of zinc uptake when 10 mM DEPC was included in the uptake

dx.doi.org/10.1021/bi201553p | *Biochemistry* 2012, 51, 963–973

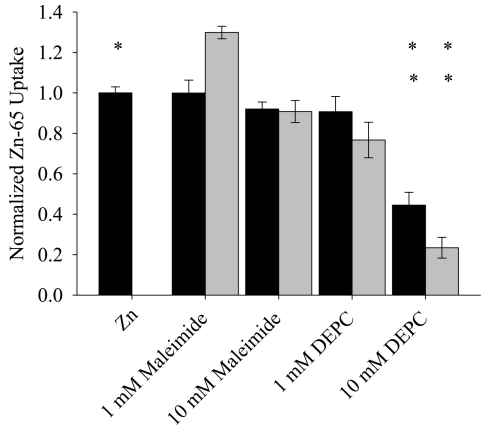

Figure 7. Extracellular residues involved in zinc translocation. To identify residues that are either directly or indirectly involved in zinc translocation, oocytes were preincubated with varying amounts of maleimide or DEPC for 30 min. Half of the oocytes were washed thoroughly to remove the labeling reagent. The uptake assay was initiated by incubation of oocytes with 6.0 μM $^{65}ZnCl_2$ for 1 h. The data were normalized to oocytes expressing hZIP4 that were not labeled with either maleimide or DEPC. Black bars represent data for zinc uptake after labeling reagents were removed prior to the uptake assay. Gray bars represent the results when the labeling reagents were present during the uptake assay. At least one asterisk indicates that there is a statistically significant difference in uptake values between the experimental and control experiments by a *t* test. Two asterisks indicate a statistically significant difference in uptake values between two experimental conditions.

assay when compared to having the 10 mM DEPC washed out prior to the radioisotope uptake assay. To determine whether the addition of 10 mM DEPC had a toxic effect on oocytes, we determined the resting membrane potential of oocytes preincubated in 0 or 10 mM DEPC for 60 min using a two-electrode voltage clamp setup. No significant difference in membrane potential was observed between these two experimental conditions. It has already been demonstrated that exposure of 10 mM DEPC to oocytes overnight has no effect on the resting membrane potential of oocytes.[36]

DISCUSSION

Zinc is a required micronutrient for hundreds of cellular processes.[37] However, the mechanism by which zinc is transported across the plasma membrane is not well-understood. There are two classes of proteins that mediate the transport of zinc across the plasma membrane. While the Znt family of proteins functions to decrease the concentration of cytosolic zinc, the ZIP family of proteins acts to increase the cytosolic zinc levels. Most hZIP proteins have eight transmembrane domain proteins that are implicated in transporting zinc across cellular membranes.[8,38,39] Members of this family, such as hZIP4, have oftentimes first been identified by sequencing of genes implicated in a disease state.[19] While cellular localization for these proteins has been investigated, the mechanism of zinc uptake, the cation selectivity, and important residues for cation transport are areas that are not well-understood for each of these proteins.

Earlier, it was proposed that hZIP2 is a Zn^{2+}/HCO_3^- symporter.[30] Later, it was reported that another member of the zinc transporter family, ZIP8, is a HCO_3^- symporter, which transports Mn^{2+} and Cd^{2+}.[32] Therefore, considering the wide distribution of the hZIP family of proteins in human tissue and organs and their functional importance in cellular homeostasis, it is essential to directly determine the cation specificity of each member of the hZIP family of proteins. The experiments in this paper describe the first examination of the cation specificity of hZIP4, a protein that has been implicated in AE, a pediatric disease characterized by behavioral and neurological disturbances.[20] More recently, it has also been observed that hZIP4 is overexpressed in pancreatic cancer cells where the surface expression of hZIP4 directly regulates the expression of proteins associated with the onset and progression of pancreatic cancer.[21,40]

To investigate the specificity and kinetic parameters of hZIP4, we used *X. laevis* oocytes as a platform to express this protein. While oocytes do have an endogenous zinc efflux mechanism, it has previously been shown that zinc efflux is independent of the extracellular zinc concentration. This will limit zinc efflux in affecting our experimentally determined kinetic parameters.[29] We have directly demonstrated that hZIP4 can transport Zn^{2+}. Furthermore, Cu^{2+} and Ni^{2+} inhibit hZIP4-mediated zinc uptake when these cations are present in micromolar amounts. In contrast, divalent cations Ba^{2+}, Cd^{2+}, Co^{2+}, Fe^{2+}, Mg^{2+}, and Mn^{2+} had no significant effect on $^{65}Zn^{2+}$ uptake. While these data are inconsistent with previous data that suggested that the mZIP4 protein is a Zn^{2+} cation transporter, it has been recently suggested that the ZIP family of proteins may have broader substrate translocation capability because hZIP14 can transport a variety of divalent cations.[11,15] Furthermore, it is important to note that from our experiments we can conclude only that Ba^{2+}, Cd^{2+}, Co^{2+}, Fe^{2+}, Mg^{2+}, and Mn^{2+} do not inhibit hZIP4-mediated $^{65}Zn^{2+}$ uptake. We cannot reach any conclusions about whether these cations can be transported by hZIP4. It has been shown that Fe^{2+} does not inhibit hZIP14-mediated $^{109}Cd^{2+}$ uptake, but that Fe^{2+} can be transported by hZIP14.[11] Therefore, it is possible that hZIP4 could mediate the transport of one of the cations mentioned above that does not inhibit $^{65}Zn^{2+}$ transport. For example, if there are multiple mechanisms for cation translocation that do not compete with each other, we would expect similar results as in Figure 3 for the cations that do not inhibit $^{65}Zn^{2+}$ uptake. Alternatively, if the rate of transport for one of these cations is sufficiently fast that it would not inhibit $^{65}Zn^{2+}$ uptake, we would also observe no change in $^{65}Zn^{2+}$ uptake upon addition of this cation in our cation competition experiment. Our subsequent experiments have demonstrated that both Cu^{2+} and Ni^{2+} can be transported by hZIP4 when these cations are present in micromolar quantities. The apparent affinities for each of these cations are in the low micromolar range.

A careful analysis of our experimental results has also uncovered a second nanomolar binding affinity for $^{65}Zn^{2+}$, $^{63}Ni^{2+}$, and $^{64}Cu^{2+}$. At this concentration, $^{65}Zn^{2+}$ and $^{64}Cu^{2+}$ are transported by hZIP4 as shown by the increase in the rate of radioisotope uptake over time. In contrast, $^{63}Ni^{2+}$ has a nanomolar binding affinity but does not appear to be transported as there is no increase in the rate of radioisotope uptake over time. Combined, these data suggest that there are at least two distinct coordination sites within hZIP4. The simplest explanation is that the high affinity for each cation is for one site while the low affinity is for a second cation coordinating site. However, our data cannot directly resolve whether this is the case. More importantly, a variety of groups have determined that the free concentration of zinc in cells is between 5 pM and 1 nM, while the free zinc concentration in plasma is estimated to be between ~0.1 and 1 nM.[41,42] Therefore, the high-affinity site could be physiologically relevant. This is an unresolved question that would require further experiments both in vivo and in vitro.

Alternatively, it could be possible that our observed increase in radioactivity over time at low concentrations of copper(II) and zinc is due to a long time course of cation binding to hZIP4. We consider this unlikely as this would likely be observed in our nickel uptake assay in the nanomolar concentration range. Therefore, on the basis of our experimental results, it appears that zinc and copper(II) can be transported at low concentrations, while the coordination of nickel does not result in transport; hence, there is no increase in the rate of nickel uptake over time (Figure 4A).

It is interesting to further examine the observation that low concentrations of $^{63}Ni^{2+}$ bind but are not transported by hZIP4 is interesting. In contrast to either Zn^{2+} or Cu^{2+}, there is no cooperativity for Ni^{2+} in the nanomolar range. We propose that there is a coordination geometry in which the binding of nickel does not lead to translocation but in which both copper and zinc can be released for transport. Nickel(II) prefers an octahedral coordination geometry, while zinc(II) and copper(II) prefer tetrahedral and tetragonal coordination geometries, respectively.[43] Perhaps the transport of nickel(II) in the nanomolar concentration range is blocked because of differences in coordination geometry.[43]

It is important to note that an analysis of our data cannot exclude other possibilities. One possibility is that nickel coordinates to a regulatory site and not a putative transport site as this would result in no nickel transport. Alternatively, the nanomolar affinity site might require a conformational change for subsequent cation translocation. If both copper(II) and zinc coordination induces a sufficient conformational change to promote translocation, whereas coordination of nickel does not induce a sufficient conformational change for cation translocation, a similar experimental result would be observed. In any event, further experiments will be required to elucidate the molecular mechanism of cation binding and transport mediated by hZIP4.

Finally, considering that zinc was originally hypothesized to be cotransported by either histidine or cysteine residues, our objective during the course of our next set of experiments was to determine whether covalent labeling of either of these residues would inhibit $^{65}Zn^{2+}$ uptake. Our data suggest that freely accessible cysteine residues, which are on the extracellular side of the protein, are not rate-limiting in $^{65}Zn^{2+}$ uptake as transport is not inhibited upon addition of high concentrations of maleimide (Figure 6). In contrast, addition of DEPC prior to the uptake assay has a significant effect on $^{65}Zn^{2+}$ uptake. This suggests that histidine residues, on the extracellular side of the protein, contribute to the transport of zinc across the plasma membrane. It is important to note here that DEPC may label histidine residues that are water accessible, but within the transmembrane domains. When DEPC is incubated with hZIP4-injected oocytes, both before and during the uptake assay when compared to washing out DEPC prior to the uptake assay, there is an added decrease in the rate of zinc uptake. We speculate that this added decrease in the rate of zinc uptake is due to a conformational change in hZIP4 that exposes one or more previously inaccessible histidine residues for labeling. Alternatively, labeling of histidine residues may "lock" hZIP4 in a conformation where further zinc uptake is not possible. A hydropathy analysis of the hZIP4 gene sequence shows that there are seven extracellular histidine residues, while the transmembrane domains encode four additional histidine residues (Figure 1). DEPC labeling of one or more of these residues contributes to the decline in the rate of zinc uptake under our experimental conditions.

It is worthwhile to use the results from these experiments to speculate about the mechanism of cation selectivity of hZIP4. The ionic radii of Ni^{2+}, Cu^{2+}, and Zn^{2+} are 83, 87, and 88 pm, respectively. Each of the other cations tested is either smaller (Fe^{2+}, 75 pm; Co^{2+}, 79 pm; Mn^{2+}, 81 pm) or larger (Cd^{2+}, 109 pm; Ba^{2+}, 149 pm) than the three cations that are transported by hZIP4, the notable exception being Mg^{2+} (86 pm). However, whereas the preferred donor atom for Mg^{2+} is oxygen, the preferred donor atoms for Ni^{2+}, Cu^{2+}, and Zn^{2+} are either sulfur or nitrogen. Our covalent modification experiments with DEPC support our proposal that histidine residues contribute to coordinating these cations and could be involved in cation translocation. This speculation should be used cautiously as the ionic radii described above are for dehydrated ions. Hydration of these transition metals during translocation would change an analysis of our results.

In conclusion, our study reveals that hZIP4 is a metal ion transporter that can transport Zn^{2+}, Ni^{2+}, and Cu^{2+}. Transport is either directly or indirectly mediated by accessible extracellular histidine residues. Our results, combined with those of other laboratories, suggest that the ZIP family of proteins has a more diverse set of substrates than originally postulated and that to understand the functional significance of each of these proteins, it may be useful to directly measure transport for each member of the ZIP family of proteins. However, it is important to acknowledge that our experiments have not been performed in the native environment of hZIP4, and thus, we must be careful in translating our results to physiological function. In vivo, it is worth noting that mutations in hZIP4 result in a zinc deficiency disease and mutations in the copper transport protein (CTR) family result in copper deficiency diseases.[44] Therefore, while hZIP4 is unlikely to be a main avenue of cellular copper uptake, hZIP4 is essential for maintaining the cellular homeostasis of zinc.

AUTHOR INFORMATION

Corresponding Author

*Department of Chemistry and Biochemistry, Worcester Polytechnic Institute, 100 Institute Rd., Worcester, MA 01605. Fax: (508) 831-4116. Telephone: (508) 831-4193. E-mail: rdempski@wpi.edu.

Funding

This study was supported by the WPI Research Foundation.

Notes

The authors declare no competing financial interest.

ACKNOWLEDGMENTS

We thank Olga Gaiko, Ryan Richards, and Tuong-Vi Nguyen for their help in the laboratory and for invaluable discussions. We are also indebted to the Gaudette laboratory for assistance with fluorescence microscopy.

ABBREVIATIONS

DEPC, diethylpyrocarbonate; HEPES, 4-(2-hydroxyethyl)-1-piperazineethanesulfonic acid; MOPS, 3-(*N*-morpholino)-propanesulfonic acid; AE, *acrodermatitis enteropathica*; PBS, phosphate-buffered saline; SEM, standard error of the mean.

REFERENCES

(1) Busch, D. H. (1995) Catalysis in Bioinorganic Chemistry. *Trans. Kans. Acad. Sci. 98*, 2−16.

(2) Brown, K. H., Wuehler, S. E., and Peerson, J. M. (2001) The importance of zinc in human nutrition and estimation of the global prevalence of zinc deficiency. *Food Nutr. Bull. 22*, 113−125.
(3) Maret, W., and Li, Y. (2009) Coordination dynamics of zinc in proteins. *Chem. Rev. 109*, 4682−4707.
(4) Hughes, M. M. N. (1991) Metal speciation and microbial growth: The hard (and soft) facts. *J. Gen. Microbiol. 137*, 725−734.
(5) Andreini, C., Banci, L., Bertini, I., and Rosato, A. (2006) Counting the zinc-proteins encoded in the human genome. *J. Proteome Res. 5*, 196−201.
(6) Liuzzi, J. P., and Cousins, R. J. (2004) Mammalian zinc transporters. *Annu. Rev. Nutr. 24*, 151−172.
(7) Ripa, S., and Ripa, R. (1995) Zinc cellular traffic: Physiopathological considerations. *Minerva Med. 86*, 37−43.
(8) Cousins, R. J., Liuzzi, J. P., and Lichten, L. A. (2006) Mammalian zinc transport, trafficking, and signals. *J. Biol. Chem. 281*, 24085−24089.
(9) Fukada, T., and Kambe, T. (2011) Molecular and genetic features of zinc transporters in physiology and pathogenesis. *Metallomics 3*, 662−674.
(10) Lu, M., and Fu, D. (2007) Structure of the zinc transporter YiiP. *Science 317*, 1746−1748.
(11) Pinilla-Tenas, J. J., Sparkman, B. K., Shawki, A., Illing, A. C., Mitchell, C. J., Zhao, N., Liuzzi, J. P., Cousins, R. J., Knutson, M. D., and Mackenzie, B. (2011) Zip14 is a complex broad-scope metal-ion transporter whose functional properties support roles in the cellular uptake of zinc and nontransferrin-bound iron. *Am. J. Physiol. 301*, C862−C871.
(12) Liu, Z., Li, H., Soleimani, M., Girijashanker, K., Reed, J. M., He, L., Dalton, T. P., and Nebert, D. W. (2008) Cd^{2+} versus Zn^{2+} uptake by the ZIP8 HCO_3-dependent symporter: Kinetics, electrogenicity and trafficking. *Biochem. Biophys. Res. Commun. 365*, 814−820.
(13) Bin, B. H., Fukada, T., Hosaka, T., Yamasaki, S., Ohashi, W., Hojyo, S., Miyai, T., Nishida, K., Yokoyama, S., and Hirano, T. (2011) Biochemical characterization of human ZIP13 protein: A homo-dimerized zinc transporter involved in the spondylocheiro dysplastic Ehlers-Danlos syndrome. *J. Biol. Chem. 286*, 40255−40265.
(14) Lin, W., Chai, J., Love, J., and Fu, D. (2010) Selective electrodiffusion of zinc ions in a Zrt-, Irt-like protein, ZIPB. *J. Biol. Chem. 285*, 39013−39020.
(15) Dufner-Beattie, J., Wang, F., Kuo, Y. M., Gitschier, J., Eide, D., and Andrews, G. K. (2003) The acrodermatitis enteropathica gene ZIP4 encodes a tissue-specific, zinc regulated zinc transporter in mice. *J. Biol. Chem. 278*, 33474−33481.
(16) Eide, D. J. (2004) The SLC39 family of metal ion transporters. *Pfluegers Arch. 447*, 796−800.
(17) Kambe, T., and Andrews, G. K. (2009) Novel proteolytic processing of the ectodomain of the zinc transporter ZIP4 (SLC39A4) during zinc deficiency is inhibited by acrodermatitis enteropathica mutations. *Mol. Cell. Biol. 29*, 129−139.
(18) Mao, X., Kim, B. E., Wang, F., Eide, D. J., and Petris, M. J. (2007) A histidine-rich cluster mediates the ubiquitination and degradation of the human zinc transporter, hZIP4, and protects against zinc cytotoxicity. *J. Biol. Chem. 282*, 6992−7000.
(19) Wang, K., Zhou, B., Kuo, Y. M., Zemansky, J., and Gitschier, J. (2002) A novel member of a zinc transporter family is defective in acrodermatitis enteropathica. *Am. J. Hum. Genet. 71*, 66−73.
(20) Van Wouwe, J. P. (1989) Clinical and laboratory diagnosis of acrodermatitis enteropathica. *Eur. J. Pediatr. 149*, 2−8.
(21) Li, M., Zhang, Y., Liu, Z., Bharadwaj, U., Wang, H., Wang, X., Zhang, S., Liuzzi, J. P., Chang, S. M., Cousins, R. J., et al. (2007) Aberrant expression of zinc transporter ZIP4 (SLC39A4) significantly contributes to human pancreatic cancer pathogenesis and progression. *Proc. Natl. Acad. Sci. U.S.A. 104*, 18636−18641.
(22) Zhang, Y. D., Yang, Q., Jiang, Z. M., Ma, W., Zhou, S. W., and Xie, D. R. (2011) Overall survival of patients with advanced pancreatic cancer improved with an increase in second-line chemotherapy after gemcitabine-based therapy. *JOP 12*, 131−137.
(23) Zhang, Y., Bharadwaj, U., Logsdon, C. D., Chen, C., Yao, Q., and Li, M. (2010) ZIP4 regulates pancreatic cancer cell growth by activating IL-6/STAT3 pathway through zinc finger transcription factor CREB. *Clin. Cancer Res. 16*, 1423−1430.
(24) Gray, M. J., Wey, J. S., Belcheva, A., McCarty, M. F., Trevino, J. G., Evans, D. B., Ellis, L. M., and Gallick, G. E. (2005) Neuropilin-1 suppresses tumorigenic properties in a human pancreatic adenocarcinoma cell line lacking neuropilin-1 co-receptors. *Cancer Res. 65*, 3664−3670.
(25) Takahashi, Y., Kitadai, Y., Bucana, C. D., Cleary, K. R., and Ellis, L. M. (1995) Expression of vascular endothelial growth factor and its receptor, KDR, correlates with vascularity, metastasis, and proliferation of human colon cancer. *Cancer Res. 55*, 3964−3968.
(26) Yamamoto, H., Itoh, F., Iku, S., Hosokawa, M., and Imai, K. (2001) Expression of the γ_2 chain of laminin-5 at the invasive front is associated with recurrence and poor prognosis in human esophageal squamous cell carcinoma. *Clin. Cancer Res. 7*, 896−900.
(27) Lorenz, C., Pusch, M., and Jentsch, T. J. (1996) Heteromultimeric CLC chloride channels with novel properties. *Proc. Natl. Acad. Sci. U.S.A. 92*, 13362−13366.
(28) Richards, R., and Dempski, R. E. (2011) Examining the conformational dynamics of membrane proteins in situ with site-directed fluorescence labeling. *J. Vis. Exp. 51*, 2627 DOI: doi: 10.3791/2627.
(29) Valentine, R. A., Jackson, K. A., Christie, G. R., Mathers, J. C., Taylor, P. M., and Ford, D (2007) ZnT5 variant B is a bidirectional zinc transporter and mediates zinc uptake in human intestinal Caco-2 cells. *J. Biol. Chem. 282*, 14389−14393.
(30) Gaither, L. A., and Eide, D. J. (2000) Functional expression of the human hZIP2 zinc transporter. *J. Biol. Chem. 275*, 5560−5564.
(31) Girijashanker, K., He, L., Soleimani, M., Reed, J. M., Li, H., Liu, Z., Wang, B., Dalton, T. P., and Nebert, D. W. (2008) Slc39a14 gene encodes ZIP14, a metal/bicarbonate symporter: Similarities to the ZIP8 transporter. *Mol. Pharmacol. 73*, 1413−1423.
(32) He, L., Girijashanker, K., Dalton, T. P., Reed, J., Li, H., Soleimani, M., and Nebert, D. W. (2006) ZIP8, member of the solute-carrier-39 (SLC39) metal-transporter family: Characterization of transporter properties. *Mol. Pharmacol. 70*, 171−180.
(33) Palmiter, R. D., and Findley, S. D. (1995) Cloning and functional characterization of a mammalian zinc transporter that confers resistance to zinc. *EMBO J. 14*, 639−649.
(34) Dahl, G., Levine, E., Rabadan-Diehl, C., and Werner, R. (1991) Cell/cell channel formation involves disulfide exchange. *Eur. J. Biochem. 197*, 141−144.
(35) Sheng, S., Perry, C. J., and Kleyman, T. R. (2002) External nickel inhibits epithelial sodium channel by binding to histidine residues within the extracellular domains of α and γ subunits and reducing channel open probability. *J. Biol. Chem. 277*, 50098−50111.
(36) Clarke, C. E., Benham, C. D., Bridges, A., George, A. R., and Meadows, H. J. (2000) Mutation of histidine 286 of the human P2X4 purinoceptor removes extracellular pH sensitivity. *J. Physiol. 523* (Part 3), 697−703.
(37) MacDonald, R. S. (2000) The role of zinc in growth and cell proliferation. *J. Nutr. 130*, 1500S−1508S.
(38) Gaither, L. A., and Eide, D. J. (2001) Eukaryotic zinc transporters and their regulation. *BioMetals 14*, 251−270.
(39) Taylor, K. M., and Nicholson, R. I. (2003) The LZT proteins; the LIV-1 subfamily of zinc transporters. *Biochim. Biophys. Acta 1611*, 16−30.
(40) Donahue, T., and Hines, O. J. (2010) The ZIP4 pathway in pancreatic cancer. *Cancer Biol. Ther. 9*, 243−245.
(41) Reyes, J. G. (1996) Zinc transport in mammalian cells. *Am. J. Physiol. 270*, C401−C410.
(42) Costello, L. C., Fenselau, C. C., and Franklin, R. B. (2011) Evidence for operation of the direct zinc ligand exchange mechanism for trafficking, transport, and reactivity of zinc in mammalian cells. *J. Inorg. Biochem. 105*, 589−599.

(43) Frausto da Silva, J. J. R., and Williams, R. J. P. (2001) *The biological chemistry of the elements: The inorganic chemistry of life*, Oxford University Press, New York.
(44) Gupta, A., and Lutsenko, S. (2009) Human copper transporters: Mechanism, role in human diseases and therapeutic potential. *Future Med. Chem. 1*, 1125−1142.